Rostami, F; Yazdi, S. R. Sabbagh; Shahrokhi, M.; Said, Azlin; Bin Abdullah, Rozi

Numerical Investigation of Velocity Profile in Hydraulic Jump Stilling Basin with VOF

Proceedings of ninth International Conference on Hydro-Science and Engineering (ICHE 2010), IIT Madras, Chennai, India.
2 - 5 August 2010

Numerical Investigation of Velocity Profile in Hydraulic Jump Stilling Basin with VOF

Rostami F. [1], S.R. Sabbagh Yazdi[2], M. Shahrokhi [3],
Md Azlin Md Said [4], Rozi Bin Abdullah[5]

Abstract: *The Hydraulic jump stilling basin is the most common form of energy dissipater that converting the supercritical flow from the spillway into subcritical flow compatible with the downstream river regime by hydraulic jump. This paper starts by giving briefly insight into the dynamics of the flow and discussing mathematical description of aerated flow as well as the turbulent models that are suitable for numerical solution of hydraulic jump. Numerical simulations undertaken in present three dimensional work use k-ε and RNG turbulent models. Results are compared with observations of mean flow. The next step of present study is using the chosen turbulent model for simulate a real stilling basin. This numerical study has been performed to predict the flow surface height and velocity distribution in the stilling basin. A commercially known software, FLOW-3D, was applied to numerically solve the Navier-Stokes equations for solution domain. The calculated results such as velocities and surface height were compared with the physical model data where available. In conclusion, the results of RNG turbulent model are better agreement with the measured data in comparison with k-ε. The results from numerical simulation of stilling basin are generally good agreed with the existing data and flow information such as velocity distribution and surface height distribution is obtained to be used for engineering design purpose.*

Keywords: *Numerical Simulation; Hydraulic Jump; Stilling Basin; Turbulent Model; VOF*

INTRODUCTION

In open channels, the transition from supercritical to sub-critical flow (i.e. a hydraulic Jump) is characterized by a sharp rise in free-surface elevation, strong turbulence, water splashing and air entrainment in the roller. Hydraulic jump is a very useful phenomenon to dissipate flow energy. Hydraulic jump is an interested phenomena for many researches (e.g. Rajaratnam (1967); Hager, Bremen and Kawagoshi (1990); Hager and Li, (1992) and Novak (1955)).

---

1 PhD Student, School of civil Engineering, Universiti Sainse Malaysia, Engineering Campus, 14300 Nibong Tebal, Seberang Perai Selatan, Palau Pinang, Malaysia, Email: fa.rostami@gmail.com
2 Assoc. Professor, Civil Engineering Department, K.N. Toosi University of Technology, No.1346 Valiasr Street, 19697- Tehran, IRAN, Email: SYazdi@kntu.ac.ir
3 PhD Student, School of civil Engineering, Universiti Sainse Malaysia, Engineering Campus, 14300 Nibong Tebal, Seberang Perai Selatan, Palau Pinang, Malaysia, Email: mshotm2000@yahoo.com
4 Assoc. Professor, School of civil Engineering, Universiti Sainse Malaysia, Engineering Campus, 14300 Nibong Tebal, Seberang Perai Selatan, Palau Pinang, Malaysia, Email: azlin@eng.usm.my
5 Assoc. Professor, School of civil Engineering, Universiti Sainse Malaysia, Engineering Campus, 14300 Nibong Tebal, Seberang Perai Selatan, Palau Pinang, Malaysia, Email: cerozi@eng.usm.my

Air entrainment in hydraulic jump was investigated as term of the air request, i.e. the total quantity of entrained air (e.g. Wood, 1990; Chanson, 1997). Resch and Leutheusser (1972) showed the air entrainment process, the energy dissipation and momentum transfer (influence of inflow condition) for first time. Recently, Chanson studied the air-water properties in partially-developed hydraulic jumps and he showed a similarity with plunging jet entrainment (Chanson and Qiao, 1994; Chanson, 1995).

The notable characteristics of hydraulic jumps can be summarized as follows: a) important turbulence intensities (often called macro turbulence); b) strong curvature of streamlines (i.e., non-hydrostatic pressure distribution); c) noticeable air entrainment into the water column through the free surface; and d) presence of a roller of horizontal axis in the upper portion of the flow. Notwithstanding the general concept of the hydraulic jump is a well-known flow phenomenon, detailed theoretical and numerical models of the internal flow features in hydraulic jumps, for all Froude numbers, have yet to be developed.

Some of the few exceptionally successful, existing theoretical models (Madsen and Svendsen, 1983; McCorquodale and Khalifa, 1981; Svendsen and Kirby, 2004) are able to estimate the velocity distribution in the vertical direction. The free surface location, and the length of hydraulic jumps, but they are unable of providing either the details of turbulence or the entrainment of air at the free surface. Recent interesting numerical results (Stelling and Busnelli, 2001; Ma et al., 2002), show adequate predictions of mean flow and turbulence, but they have not considered the two-phase nature of the flow and then air entrainment. Ma et al. (2002) stated in their efficient, recent numerical simulation of a submerged hydraulic jump "it is expected that the inclusion of air entraining, the effect of streamline curvature and more accurate free surface conditions for turbulent quantities would improve the numerical calculation of hydraulic jumps significantly."

The maximum turbulence intensities and Reynolds stress at any section decrease from the toe of the jump towards downstream the jump rapidly and then gradually level off in the transition region from the end of the jump to the friction dominated open channel flow downstream. The maximum turbulence kinetic energy at each section decreases linearly with the longitudinal distance within the jump and gradually levels off in the transition region (Liu, et al., 2004).

The objective of this paper is to characterize mean flow and air entrainment in hydraulic jumps through numerical means (FLOW-3D®), in three dimensions, using the one-phase flow theory. In this endeavor, the code does not incorporate any assumption about hydrostaticity (i.e., "streamline curvature" is considered explicitly); it embeds a very accurate treatment for the free surface through the true VOF (volume-of-fluid) method. The global, aim of this work is to obtain a set of validated turbulent model for hydraulic jumps for different Froude numbers.

AERATED FLOW MATHEMATICAL MODEL

Time averaged flow equations

The general mass continuity equation is (Flow-3D, Ver.9.1):

$$V_f \frac{\partial \rho}{\partial t} + \frac{\partial}{\partial x}(\rho u A_x) + \frac{\partial}{\partial y}(\rho v A_y) + \frac{\partial}{\partial z}(\rho w A_z) = 0 \tag{1}$$

Where V_f is the fractional volume open to flow, ρ is the fluid density. The velocity components (u,v,w) are in the coordinate directions (x,y,z). A_x, A_y and A_z are similar area fractions for flow in the *x, y* and *z* directions, respectively. The equation of motion for the fluid velocity components in the three directions are the Navier – Stokes equations (Flow-3D, Ver.9.1):

$$\frac{\partial u}{\partial t} + \frac{1}{V_F}\left\{uA_x \frac{\partial u}{\partial x} + vA_y R\frac{\partial u}{\partial y} + wA_z \frac{\partial u}{\partial z}\right\} = -\frac{1}{\rho}\frac{\partial p}{\partial x} + G_x + f_x \tag{2}$$

$$\frac{\partial v}{\partial t} + \frac{1}{V_F}\left\{uA_x \frac{\partial v}{\partial x} + vA_y R\frac{\partial v}{\partial y} + wA_z \frac{\partial v}{\partial z}\right\} = -\frac{1}{\rho}\left(R\frac{\partial p}{\partial y}\right) + G_y + f_y \tag{3}$$

$$\frac{\partial w}{\partial t} + \frac{1}{V_F}\left\{uA_x \frac{\partial w}{\partial x} + vA_y R\frac{\partial w}{\partial y} + wA_z \frac{\partial w}{\partial z}\right\} = -\frac{1}{\rho}\frac{\partial p}{\partial z} + G_z + f_z \tag{4}$$

In these equations, G_x, G_y, G_z are body accelerations, and f_x, f_y, f_z are viscous accelerations that for a variable dynamic viscosity μ are as follows:

$$\rho V_F f_x = wsx - \left\{\frac{\partial}{\partial x}(A_x \tau_{xx}) + R\frac{\partial}{\partial y}(A_y \tau_{xy}) + \frac{\partial}{\partial z}(A_z \tau_{xz}) + \frac{\xi}{x}(A_x \tau_{xx} - A_y \tau_{yy})\right\} \tag{5}$$

$$\rho V_F f_y = wsy - \left\{\frac{\partial}{\partial x}(A_x \tau_{xy}) + R\frac{\partial}{\partial y}(A_y \tau_{yy}) + \frac{\partial}{\partial z}(A_z \tau_{yz}) + \frac{\xi}{x}(A_x - A_y \tau_{xy})\right\} \tag{6}$$

$$\rho V_F f_z = wsz - \left\{\frac{\partial}{\partial x}(A_x \tau_{xz}) + R\frac{\partial}{\partial y}(A_y \tau_{zy}) + \frac{\partial}{\partial z}(A_z \tau_{zz}) + \frac{\xi}{x}(A_z - A_y \tau_{xz})\right\} \tag{7}$$

Where:

$$\tau_{xx} = -2\mu\{\frac{\partial u}{\partial x} - \frac{1}{3}(\frac{\partial u}{\partial x} + \frac{\partial v}{\partial y} + \frac{\partial w}{\partial z})\},\ \tau_{yy} = -2\mu\{\frac{\partial v}{\partial y} - \frac{1}{3}(\frac{\partial u}{\partial x} + \frac{\partial v}{\partial y} + \frac{\partial w}{\partial z})\},\ \tau_{zz} = -2\mu\{\frac{\partial w}{\partial z} - \frac{1}{3}(\frac{\partial u}{\partial x} + \frac{\partial v}{\partial y} + \frac{\partial w}{\partial z})\}$$

$$\tau_{xy} = -\mu\{\frac{\partial v}{\partial y} + \frac{\partial u}{\partial x}\},\ \tau_{xz} = -\mu\{\frac{\partial u}{\partial z} + \frac{\partial w}{\partial x}\},\ \tau_{yz} = -\mu\{\frac{\partial v}{\partial z} + \frac{\partial w}{\partial y}\} \tag{8}$$

Free Surface Trace Equation

Free surface boundary configuration of the flow is defined in terms of a volume of fluid (VOF) function, $F(x,y,z$ and $t)$. This function represents the volume of fluid per unit volume and satisfies the Eq. (9).

$$\frac{\partial F}{\partial t} + \frac{1}{V_F}\left[\frac{\partial}{\partial x}(FA_x u)\frac{\partial}{\partial y}(FA_y v) + \frac{\partial}{\partial z}(FA_z w)\right] = 0 \tag{9}$$

The interpretation of F depends on the type of problem being solved. For a single fluid, F represents the volume fraction occupied by the fluid. Thus fluid exists where F=1 and void regions correspond to locations where F=0. Voids are regions without fluid mass that have a uniform pressure assigned to them. Physically they represent regions filled with a vapor or gas whose density is insignificant with respect to fluid density.

Air entrainment relations

Air entrainment at water surface is found on the conception that turbulent eddies lift small water segments above a free surface that may trap air and carry it back into the liquid. The extent to which water elements can be raised above a free surface depends on whether or not the intensity of the turbulence is enough to affect the surface stabilizing forces of gravity and surface tension (Flow-3D, Ver.9.1).

Turbulent kinetic energy, Q, and dissipation functions, D, are characters of the turbulence transport models. A characteristic size of turbulence eddies is then given by Eq. (10).

$$L_t = cnu(3/2)^{1/2} Q^{3/2} D \qquad (10)$$

This scale is used to distinguish surface interface. The turbulence kinetic energy per unit volume (i.e., pressure), connected to fluid element lifted to a height height L_t and with surface tension energy based on a curvature of L_t:

$$P_d = \rho g_n L_t + \sigma / L_t \qquad (11)$$

Here ρ is the liquid density, σ its coefficient of surface tension, and g_n is the component of gravity normal to the free surface (Flow-3D, Ver.9.1). Air entrainment will occur when the turbulent kinetic energy per unit volume, $P_t=\rho Q$, is larger than P_d, i.e., the turbulent disturbances must be large enough to overcome the surface stabilizing forces.

The volume of air entrained per unit time, δV, should be proportional to the surface area, A_s, and the height of the disturbances above the mean surface level. All together, we write $\delta V = C_{air} A_s \sqrt{(2(P_t - P_d)/\rho)}$, where C_{air} is a coefficient of proportionality. If P_t is less than Pd then δV is zero. The value of C_{air} is expected to be less that unity, because only a portion of the raised disturbance volume is occupied by air. A good first guess is C_{air}=0.5, i.e., assume on average that air will be trapped over about half the surface area (Flow-3D, Ver.9.1).

TURBULENT MODELS

k-ε and RNG turbulent models were used in this study and their results are compared with the experimental measurements in the next sections.

k-ε turbulent model

The simplest model consists of a transport equation for the specific kinetic energy associated with turbulent velocity fluctuations plus a parameter that characterizes some other property of the turbulence. The choice of parameters is arbitrary provided it can be used with the kinetic energy to determine length and time scales characterizing the turbulence.

A slightly more advanced (and more widely used) model consists of two transport equations for the turbulent kinetic energy k and its dissipation ε, the so-called *k-ε* model (Harlow and Nakayama, 1967). The *k*- ε model has been shown to provide reasonable approximations to many types of flows, although it sometimes requires modification of its dimensionless parameters (or even functional changes to terms in the equations) (Svendsen and Kirby,2004). The turbulence kinetic energy, k, and its rate of dissipation, ε, are obtained from the following transport equations:

$$\frac{\partial k}{\partial t}+\frac{1}{V_F}\left\{uA_x\frac{\partial k}{\partial x}+vA_y\frac{\partial k}{\partial y}+wA_z\frac{\partial k}{\partial z}\right\}=P+G+Diff-\varepsilon \tag{9}$$

$$\frac{\partial \varepsilon}{\partial t}+\frac{1}{V_F}\left\{uA_x\frac{\partial \varepsilon}{\partial x}+vA_y\frac{\partial \varepsilon}{\partial y}+wA_z\frac{\partial \varepsilon}{\partial z}\right\}=\frac{C_{1\varepsilon}.\varepsilon}{k}\left(P+C_{3\varepsilon}.G\right)+DDif-C_{2\varepsilon}.\frac{\varepsilon^2}{k} \tag{10}$$

Where, P is shear production, G is buoyancy production, *Diff* and *DDif* represent diffusion and $C_{1\varepsilon}$, $C_{2\varepsilon}$, $C_{3\varepsilon}$ are constant. In standard k-ε model $C_{1\varepsilon}$=1.44 and $C_{2\varepsilon}$=1.92.

RNG turbulent model

Another, more recent turbulence model is based on Renormalization-Group (RNG) methods (Yakhot and Orszag, 1986 and Yakhot and Smith, 1992). This approach applies statistical methods for a derivation of the averaged equations for turbulence quantities, such as turbulent kinetic energy and its dissipation rate. The RNG-based models rely less on empirical constants while setting a framework for the derivation of a range of models at different scales.

This model uses equations similar to the equations for the k-ε model. However, equation constants that are found empirically in the standard k-ε model are derived explicitly in the RNG model. Generally, the RNG model has wider applicability than the standard k-ε model. In particular, the RNG model is known to describe more accurately in low intensity turbulence flows and flows having strong shear regions. In RNG model $C_{1\varepsilon}$=1.42 and $C_{2\varepsilon}$=1.68.

NUMERICAL SOLUTION TECHNIQUES

FLOW-3D® numerically solves the equations described in the previous sections using finite-volume approximations. The flow region is subdivided into fixed rectangular cells. With each cell, there are associated local average values of all dependent variables. All variables are located at the centers of the cells except for velocities, which are located at cell faces (staggered grid arrangement). The basic numerical method used in ***FLOW-3D®*** has a formal accuracy that is first order with respect to time and space increments. Special precautions have been taken to maintain this degree of accuracy even when the structured mesh is non-uniform.

A new VOF advection method based on a 3-D reconstruction of the fluid interface has been developed and implemented in ***FLOW-3D®*** Version 8.2. The Volume-of-Fluid (VOF) function is moved in one-step, without resorting to an operator splitting technique, which gives the present method increased accuracy when the flow is not aligned with a coordinate direction. The existing VOF advection method in ***FLOW-3D®*** is based on the donor-acceptor approach first introduced by Hirt and Nichols (1981).

VERIFICATION TEST

In this section, the experimental data for velocity profiles obtained from the plots provided by Chanson and Brattberg (2000) are used for verification of numerical simulations. The experiments were accomplished in a 3.2-m long horizontal rectangular channel. the flume was 0.25-m wide and 0.30-m depth. A controlled flow was supplied through an adjustable vertical sluice gate. During the experiments, the gate opening was fixed at 20 mm. Froude number at the inlet was considered at 6.33 and 8.48, similar to the experimental study.

The upstream boundary condition for this case, with sub-critical flow occurring at upstream boundary, with is specified upstream depth (h_0). As downstream flow is sub-critical, and water surface conditions are applied at downstream end. The k-ε and RNG models are used for turbulence modeling. A uniform mesh with 5×5×5mm size was employed.

The computed results obtained using k-ε and RNG turbulent models are compared with Chanson and Brattberg (2000) observations in Figure 1. The general agreement between predicted and measured profiles produced by RNG turbulent model is more satisfactory. However, because of highly aerated turbulent flow in the upper zone of hydraulic jump, there are poor agreements between computed and measured velocity values in the upper zone of circulation region. In addition, the prediction software is better in the case of higher Froude number.

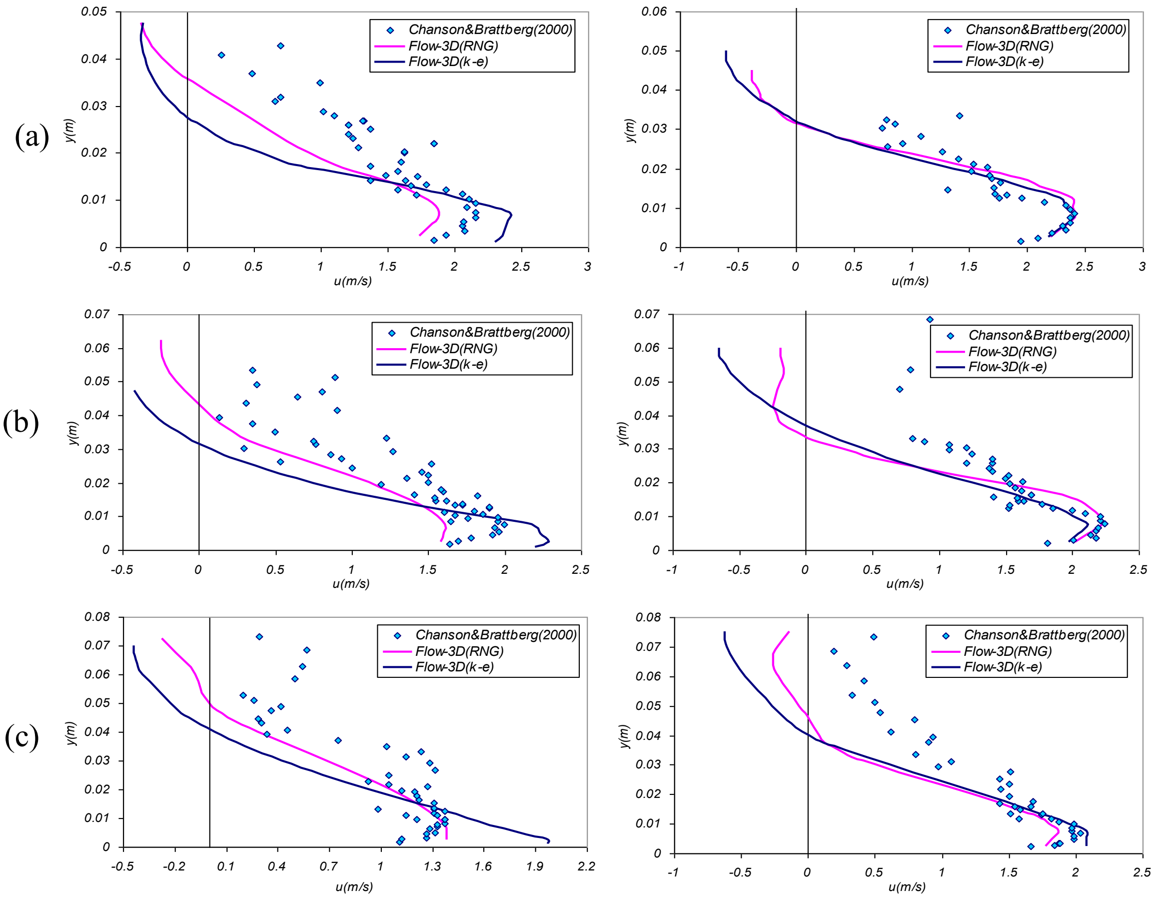

F= 6.33 F= 8.48

Fig. 1. *x*- direction velocity profile at (a) 0.05 m, (b) 0.1 m, (c) 0.2 m from toe of jump.

Figures 2 and 3 show the numerical x-direction velocity component and pressure contours for two Froude number. As expected, because of the curvature of streamlines in the circulation zone, pressure distribution in this zone is non-hydrostatic. In addition, there is negative *x*-velocity in the jump location.

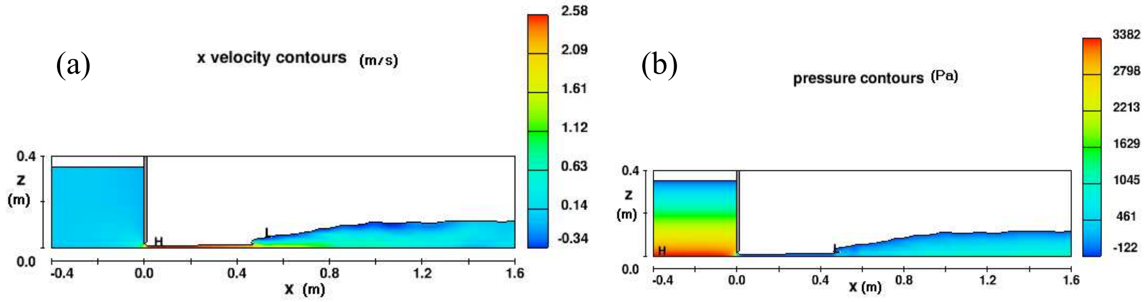

Fig. 2. (a) *x*-direction velocity and (b) Pressure contours for F=6.33 and RNG model.

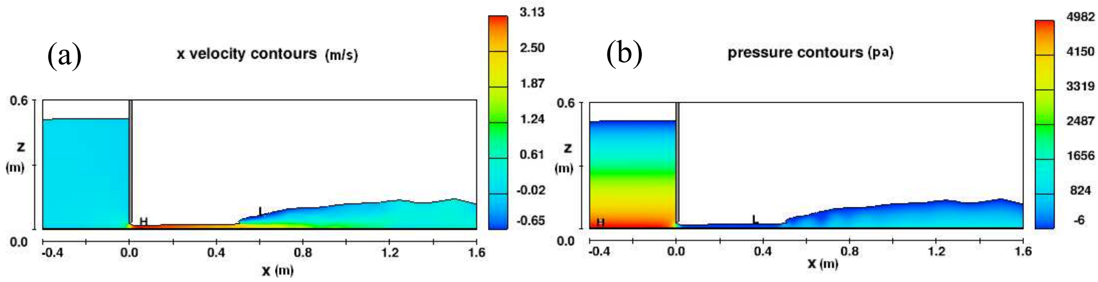

Fig. 3. (a) *x*-direction velocity and (b) Pressure contours for F=8.48 and RNG model.

MODELLING OF A HYDRAULIC JUMP STILLING BASIN

To using the software in the real project, the result of physical model of stilling basin of a reservoir dam in IRAN was considered in this study. Flood control system includes the approach channel, Ogee spillway, chute spillway and stilling basin in the right side of dam. The physical model of the flood control system was built based on the Froude similarity (scale 1:40) in Iran Water Research Institute (IWRI, 2006). Major parameter of flow like water depth, velocity and pressure was measured.

A 3-Dimensional mesh in pilot-scale was used for numerical simulations. Since Flow-3D uses FAVOR method for modeling obstacles, a good accuracy mesh block must be use for better modelling of obstacles in stilling basin. The uniform rectangular mesh with 30×30×30cm cells was applied. Moreover, a 5m band in center of basin was investigated for reducing of computational time. Detail parameter of simulated stilling basin is shown in Fig. 4.

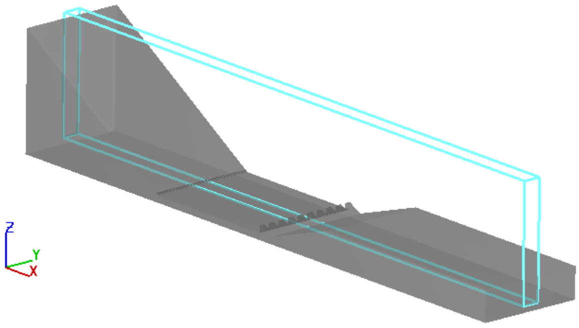

Fig. 4. An isometric view of simulated stilling basin and wedge of mesh block.

A supercritical flow with high Froude number inter the basin and if the basin works suitable, hydraulic jump dissipate the energy of flow, and a subcritical flow with low velocity exit the basin. Specified velocity and water depth was applied for inlet and outflow condition was exerted for outlet boundary condition. The basin was simulated for 1000-years, 10 000-years and PMF flood and the inlet boundary condition is shown in Table 1.

Table 1. Inlet boundary condition for upstream ob stilling basin (IWRI, 2006)

Return Period (year)	**Discharge** (m^3/s)	**Water Surface Level** (m.a.s.l)	**Velocity** (m/s)
1000	500	1428.18	29.25
10 000	830	1428.52	31.94
PMF	2270	1429.92	36.81

According to the result of simulation of hydraulic jump in previous section, the RNG turbulence model was applied for simulation of flow in the stilling basin.

Result and discussion

Available laboratory data for comparing parameters including water surface level, flow rate and bed pressure. In Fig. 5 to 8 the values that calculated by the software with the measured values have been compared.

Fig. 5 shows water surface profiles for 1000 years, 10 000 years and the PMF flood. As shown in this figure, the calculated values have a good agreement with the observations; especially computed water level after basin have converged in comparison observed surface profile. From the hydraulic point of view, there is high level of turbulence kinetic energy and energy dissipation in the first part of jump and this is why that the computed values are a little different from observed, and this interval reduce in the end of basin due to reducing the turbulence kinetic energy and energy dissipation. Simulation and experiment results show that the basin is not suitable for PMF flood, and very high super critical flow exit from the basin and basin does not work as an energy dissipater in 2270 m^3/s flood.

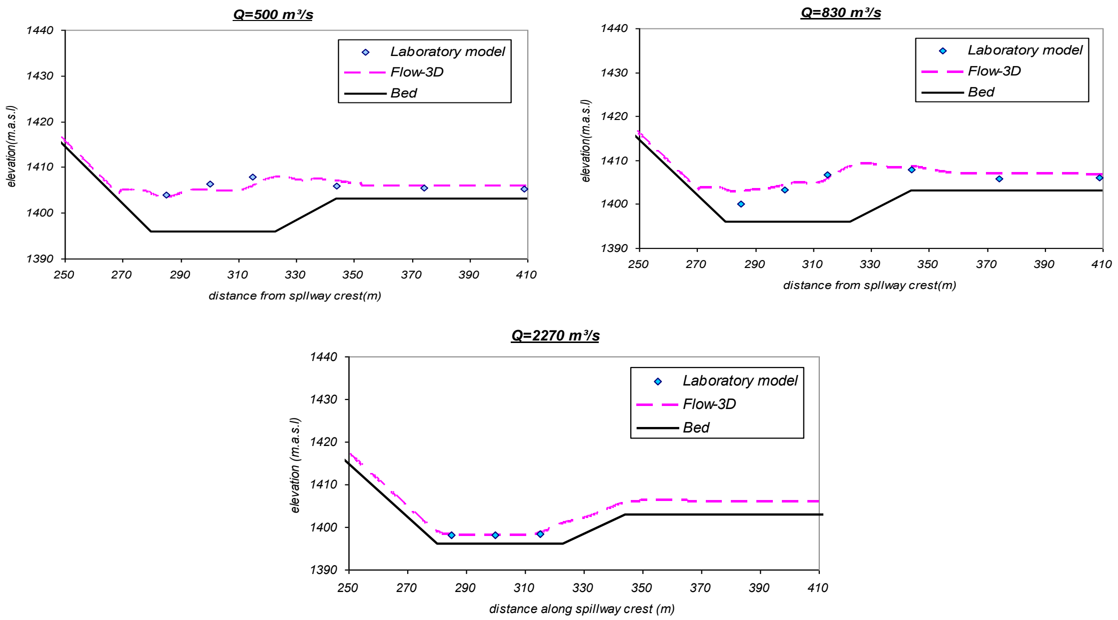

Fig. 5. Water surface profile for Q= 500, 850 and 2270 m^3/s.

The values of horizontal velocity in basin are presented in Fig. 6,7,8. Due to the current rotation in this area, the horizontal velocities near the water surface will be negative. Depth distributions of computed horizontal velocity in basin showed this phenomenon. The values of horizontal velocity near the bed and in the channel after the basin are consistent with experimental data. Moreover in the case of PMF flood (Q=2270 m^3/s) that there is not formed any hydraulic jump, computed velocity in compared of experimental value, has a good accurate.

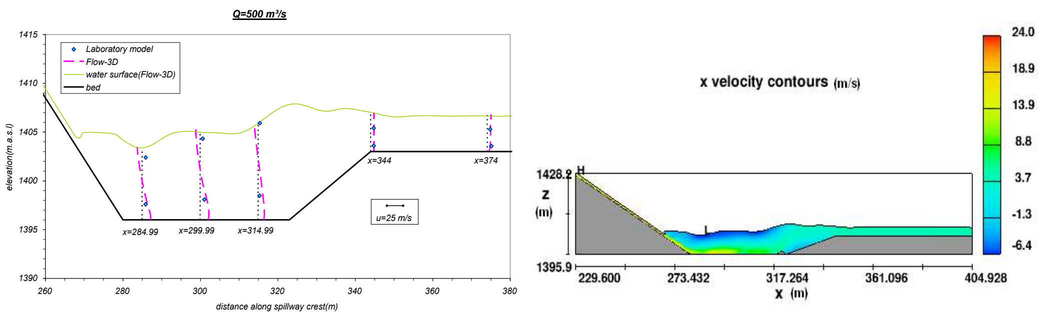

Fig. 6. x-direction velocity profile for Q = 500 m^3/s.

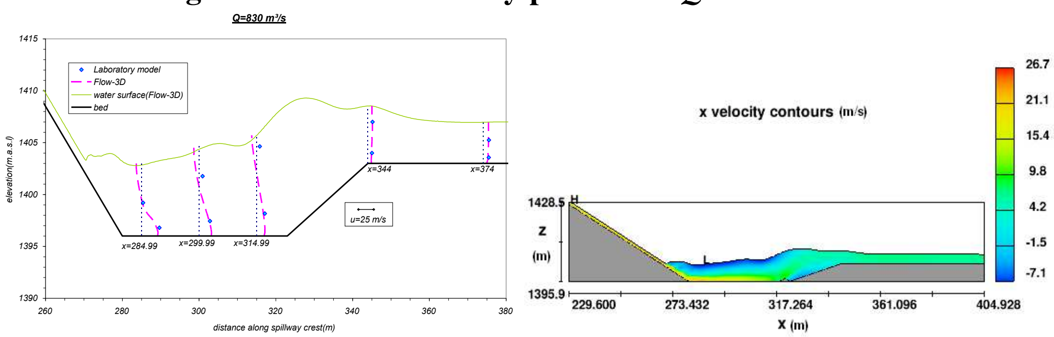

Fig. 7. x-direction velocity profile for Q = 830 m^3/s.

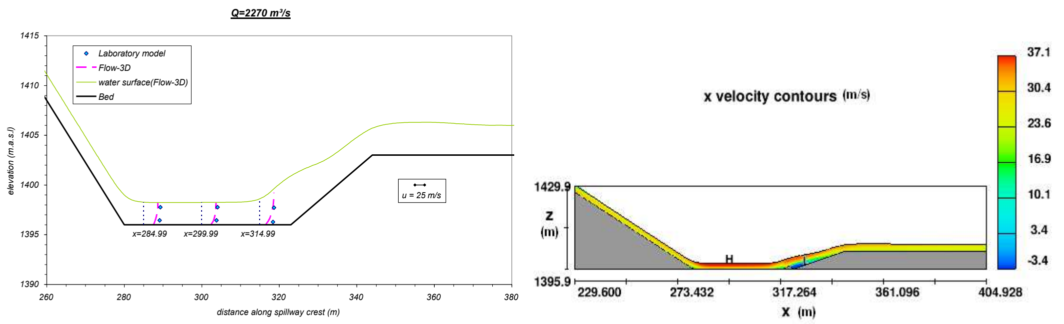

Fig. 8. ***x*-direction velocity profile for *Q* = 2270 m^3/s.**

CONCLUSION

In this paper, numerical investigations are performed for evolution of the ability of an available 3D flow solver to cope with the fully turbulent aerated flow with free surface in transition from super-critical to sub-critical flow. In this work ***FLOW-3D***® finite volume flow solver that is utilized with VOF technique, for free-surface modeling is used. The results of numerical experiments of two turbulent modeling options of the software; RNG and k-ε two equation models are used in this paper. The comparison of the computed results of two test cases of aerated hydraulic jumps with the reported experimental measurements shows that: (i)The CFD code can efficiently forecast the general trend of transformation of three dimensional velocity patterns to the horizontal velocity field. (ii) In aerated hydraulic jumps zone, the x-direction velocity trend forecasted by the RNG turbulent model present better agreement with the measured data, rather than the results produced with the k-ε turbulent model. At the lower zones of the aerated hydraulic jump the trends of computed x-direction velocity component is very similar to the experimental data, while the computed profiles x-direction velocity differ from measured data at the upper parts of aerated hydraulic jumps. However, the velocity fields computed using RNG turbulent model are slightly less than the experimental measurements at all sections in the stilling basin.

REFERENCES

Baldy, S. 1988. Bubbles in the close vicinity of breaking waves: Statistical characteristics of the generation and dispersion mechanism. *J. Geophysical Research*, 93 (1), 8239-8248.

Chanson H., Brattberg T. 2000. Experimental study of the air-water shear flow in hydraulic jump. *International Journal of Multiphase Flow*, Vol.26. 583-607.

Chanson, H. 1995. Air bubble entrainment in free-surface turbulent flows. *Experimental investigations. Report CH46/95, Department of Civil Engineering, University of Queensland, Australia,* 368.

Chanson, H. 1997. Air Bubble Entrainment in Free-surface Turbulent Shear Flows, *Academic Press, London*, UK, 401.

Chanson, H., Qiao, G.L. 1994. Air bubble entrainment and gas transfer at hydraulic jumps. *Research Report No.* CE149, Department of Civil Engineering, University of Queensland, Australia, 68.

Flow-3D® Help, Ver. 9.0, *Flow science Inc*.

Hager, W.H., Bremen, R., Kawagoshi, N. 1990. Classical hydraulic jump, Length of roller. *Journal of Hydraulic Research* 28 (5), 591-608.

Hager, W.H., Damei Li, 1992. Sill-controlled energy dissipater. *Journal of Hydraulic Research* 30 (2), 165-181.

Harlow, F.H. and Nakayama, P.I. 1967. Turbulence Transport Equations. *Phys. of Fluids,* 10.

Hirt C.W, Nichols B.D. 1981. Volume of fluid (VOF) Method for the dynamics of free boundaries. *J. of computational physics*, Vol. 39, 201-225.

IWRI (Iran Water Research Institute). 2006. Report No. HSM8403.

Liu, M., Rajaratnam, N. and. Zhu, D. 2004. Turbulence Structure of Hydraulic Jumps of Low Froude Numbers. *Journal of Hydraulic engineering*, 130(6), 511-520.

Ma, F., Hou, Y.and Prinos, P. 2002. Numerical calculation of submerged hydraulic jump. *Journal of Hydraulic Research.* vol. 39, No. 5, 1-11.

Madsen, P. and Svendsen, I. 1983. Turbulent bores and hydraulic jumps, *J. Fluid Mech*., 129, 1 1-25.

McCorquodale, J. and Khalifa, A. 1981. Internal flow in hydraulic jumps. *J. Hyd. Eng*., 109. 684-701.

Novak, P. 1955. Study of stilling basins with special regard to their end sills, *6th Congress of the International Association of Hydraulics Research*, The Hague, Paper C15.

Rajaratnam, N. 1967. Hydraulic jumps, *in Advances in Hydroscience*, Vol. 4 (ed. V.T. Chow), Academic Press, New York.

Resch, F.J., Leutheusser, H.J. 1972. The hydraulic jump: turbulence measurements in the two-phase flow region, *J. La Houille Blanche*, (4), 279-293 (in French).

Stelling, G.S., Busnelli, M.M. 2001. Numerical simulations of the vertical structure of discontinuous flows. International *Journal for Numerical Methods in Fluids.* 37 (1), 23-43.

Svendsen, I. and Kirby, J. 2004. Numerical study of a turbulent hydraulic jump. *17th ASCE Engineering Mechanics Conference,* University of Delaware, New mark.

Wood, I.R. 1990. Air entrainment in free-surface flows. *IAHR Hydraulic Structures Design Manual,* No. 4, Hydraulic Design Considerations. Balkema, Rotterdam, the Netherlands, 149.

Yakhot V. and Orszag S.A. 1986. Renormalization Group Analysis of Turbulence. I. Basic Theory. *J. Scientific Computing*, 1, 1-51.

Yakhot V. and Smith L.M. 1992. The Renormalization Group, the e-Expansion and Derivation of Turbulence Models, *J. Scientific Computing*, 7, 35-61.